Organo Opto-Electronics
*An International Journal*

http://dx.doi.org/10/18576/ooe/020101

# Optical Properties of Nano-Rods PTCDA Thin Films: an Important Material for Optoelectronic Applications

*S. AlFaify*[1,*], *Y. S. Rammah*[2], *H. Y. Zahran*[1,3], *F. Yakuphanoglu*[4] *and Mohd. Shkir*[1]

[1]Advanced Functional Materials & Optoelectronics Laboratory (AFMOL), Department of Physics, Faculty of Science, King Khalid University, P.O. Box 9004, Abha, Saudi Arabia.
[2]Physics Department, Faculty of Science, Menoufia University, Shebin El-Koom, Egypt.
[3]Metallurigical Lab., Physics Department, Faculty of Education, Ain Shams University, Roxy, Cairo, Egypt.
[4]Department of Physics, Faculty of Science and Arts, Firat University, Elazığ, Turkey.

Received: 21 Feb. 2015, Revised: 22 Mar. 2015, Accepted: 24 Mar. 2015.
Published online: 1 Jul. 2016.

**Abstract:** Thin films of 3,4,9,10-perylenetetracarboxylic dianhydride (PTCDA) of different thicknesses (155, 230, 354, and 470 nm) are prepared using thermal evaporation method. The XRD pattern confirms that the this films are preferentially grown along (102) direction. The morphology was studied by AFM and showed that the prepared films are nanocrystalline in nature consisting rod like nano-particles grains. The average grain's size was fond to be 44.5 nm with RMS (root mean square) surface roughness of 11.6 nm. The optical properties was studied in the wavelength range of 300-2600 nm. Further the collected data of transmittance T(λ) and reflectance R(λ) coefficients was used to calculate its refractive and absorption (*n* & *k*) indices. The dielectric ($\varepsilon_1$ & $\varepsilon_2$), dissipation factor ( $\tan\delta$ ), optical conductivity ( $\sigma_{opt}$ ), optical band gap ( $E_g^{opt}$ ), volume energy loss (VELF) and surface energy loss (SELF) functions are calculated and discussed. Owing to the measured optical absorption data of the film, there are four indirect band gaps ranging from 1.88 to 3.45eV. Overall, the obtained data suggests that the PTCDA film can serve as potential materials for optoelectronic devices.

**Keywords:** Organic Semiconductor, PTCDA Film, Nanostructure, Optical Parameters, Optoelectronic Devices.

## 1 Introduction

Organic semiconductors with developed conjugated $\pi$-electronic systems are commonly utilized in many optoelectronic applications as organic LED (light emitting diode) and photovoltaics. In general, organic materials excel in various aspects in comparison with their inorganic counterparts. They are low toxic materials and have technological advantages when producing effective photoconductive compounds. In addition, they are more flexible for devices fabrications (Borsenberger, 1998; Law, 1993). Moreover, some organic materials such as phthalocyanine, perylene, and their derivatives can be utilized to form complex structures. Therefore, the quasi-epitaxial orders of such material can be achieved by growing the thin films using advanced epitaxial growth techniques (Forrest, 1997). Such this films fabrication with good properties are overwhelmingly good for advanced optical technologies.

Recently, studies on the properties of PTCDA materials, in particular, structural and morphological investigations on 3,4, 9,10- Perylenetetracarboxylic dianhydride (PTCDA) were carried out (Fenter et al., 1997; Forrest, 1997; Schmitz-Hübsch et al., 1997). Such studies shows that the PTCDA materials exhibit promising properties (electrical and optical) from optoelectronic applications points of view. These properties are most probably due to the material's electronic structure as its regular planar $\pi$–$\pi$ stacking and its narrow intermolecular distance, which cause directional interactions (strong and weak) (Fenter et al., 1997; Forrest, 1997; Schmitz-Hübsch et al., 1997). Therefore, the PTCDA materials are considerably studied as a model material for organic molecular excitations. However, beside the fundamental interest in the PTCDA materials, there are another interests due to its potential applications in modern organic electronic and optoelectronic devices (Oukachmih et al., 2005), field-effect transistors (FETs) (Briseno et al., 2007; Jones et al., 2007), light-emitting diodes (LEDs) (Hoeben et al., 2005), organic semiconductors (Chen et al., 2007; Würthner et al., 2001), and in waveguides and

*Corresponding author e-mail: saalfaify@kku.edu.sa.

other microwave applications (Böhler et al., 1998; Karmann et al., 1996; Lee et al., 1998; Shen et al., 1997; Taylor et al., 1997; Urbach et al., 1998).

However, utilizing the use of the PTCDA materials in different applications requires a thorough knowledge of the material's optical properties that is still scarce. Few optical and structural data on the PTCDA and its derivatives have been seen lately in the literature including absorption spectra (Bayliss et al., 1999; Bulović et al., 1996), showing a two-peaks structure in the range of 400 to 600 nm, with a broader peak at higher-energy and narrower and less intense one at lower-energy range. The PTCDA crystallizes into two polymorphs $\alpha$ - and $\beta$ -phases in which their relative amount depends on the film thickness and the substrate temperature (Leonhardt et al., 1999; Möbus et al., 1992). The PTCDA's optical functions of the $\alpha$ - and $\beta$ -phases are unknown yet, except for the low-temperature regimes. In the literature, the reported refractive indices of the PTCDA film has been obtained for a small part (300–800 nm) of the general spectral range (Djurišić et al., 2000), or at fixed wavelength (Nagaseki et al., 1995; Zang et al., 1991). Knowledge on the optical constants of the PTCDA film is essentially important for its applications in biochemistry, biophysics, biomedicine, and optoelectronic devices. In addition, it is critical for the evaluation and standardization of the measured optical data of the film obtained by varying methods such as Raman, infrared, reflection, and anisotropy spectroscopes (Friedrich et al., 2002). Moreover, the investigation of the derivatives of 3,4,9,10-PTCDA thin films are tremendously increased for overall understanding of the growth nature of organic molecules films deposited on different substrates.

The objective of this paper is to present an investigation on the structural and optical properties of the 3,4,9,10-PTCDA thin films grown with various thicknesses. The absorption spectra were measured in a wide range of wavelengths, spanning from 300 to 2600 nm. In addition, the optical constants of the 3,4,9,10-PTCDA films, over the chosen spectral range, were determined from transmittance $T(\lambda)$ and reflectance $R(\lambda)$ measurements of the film. The transport property, onset and the fundamental energy gaps, are estimated. The complex dielectric functions and the volume/surface energy loss functions are computed. Moreover, dissipation factor and optical conductivity behaviors of the film are also studied and discussed in different sections.

## 2 Experimental Procedures

Pure raw material of 3,4,9,10- Perylenetetracarboxylic dianhydride (PTCDA) was purchased from Sigma-Aldrich company and used for thin films fabrications without any further purification. Molecular structure of PTCDA is shown in Fig. 1. Physical evaporation system was utilized to grow PTCDA films in a high vacuum coating unit (PVD-HANDY/2S-TE, Vaksis Company), with a pressure within the growth chamber reaching better than $2x10^{-5}$ torr. The PTCDA material was vacuum sublimated within a special designed Silica tube crucible heated by a boat- shaped Molybdenum.

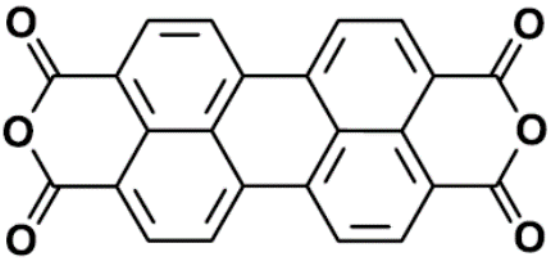

**Fig.1.** Schematic representation for the PTCDA molecular structure.

Structural investigations of the PTCDA films grown on glass substrate were carried out using X-ray diffraction (XRD)technique. Philips X-ray diffractometer (model X'-Pert) was utilized for the measurement, equipped with a monochromatic $CuK_\alpha$ radiation source operated at 40 kV and 25 mA. Diffraction patterns were recorded automatically with a scanning speed of 2°/min.

The surface morphology of the PTCDA film was also characterized using atomic force microscope (AFM), Solver-Next, NT-MDT, Russia available at the nano-labs of the physics department at King Khalid University. The analysis of the nano-grain structure and surface topology of the studied films were accomplished from the obtained AFM' micrographs using specialized software.

The transmittance *T(λ)* and reflectance *R(λ)* spectra of the as-deposited PTCDA films were measured at normal incidence of light in the spectral range of 300–2600 nm by a double-beam spectrophotometer (JASCO model V-670 UV–Vis–NIR). A

glass blank substrate was used as a reference for the transmission/reflection scans.

## 3 Results and Discussion

### *3.1 Structural investigations*

PTCDA is known to crystallize in two polymorphic forms$\alpha$ and $\beta$ depending on its growth conditions. The structure of the two phases are very similar both crystallizing in the monoclinic structure with $P_{21}/c$ space group. The lattice constants of $\alpha$-phase are $a$=3.72Å,$b$=11.96 Å and $c$= 17.34 Å while for $\beta$ -phase $a$=3.78 Å, $b$=19.30 Å and $c$= 10.77 Å within the same space group (Möbus et al., 1992). X-ray diffraction of powder and thin film (thickness ~ 470 nm) PTCDA are shown in Fig.2a. The *hkl* of each peak for the powder pattern was generated using index software depending on the values of the lattice parameters of the studied phases. The *hkl* of the studied powder pattern are more related to the $\beta$-phase.

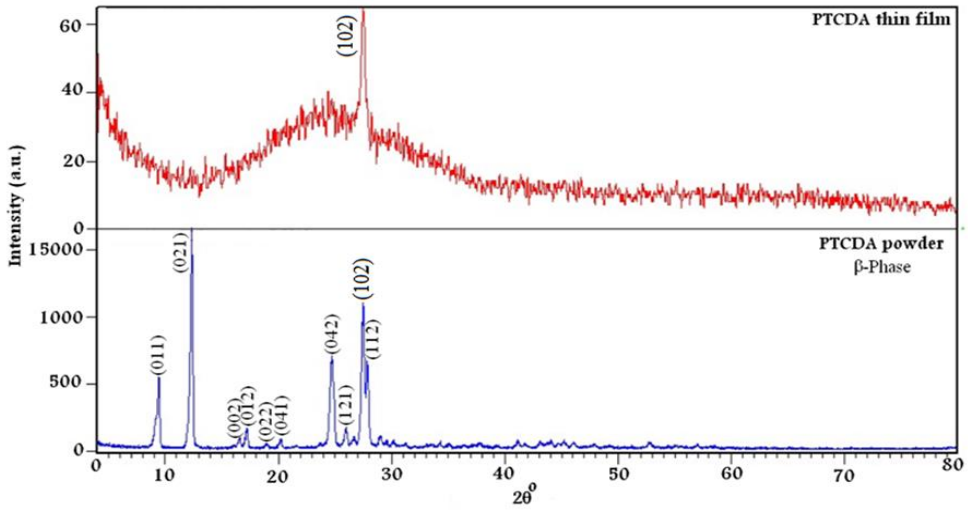


**Fig.2a.** X-ray diffraction (XRD) pattern of the PTCDA powder and thin film with thickness 470 nm (as a representative example).

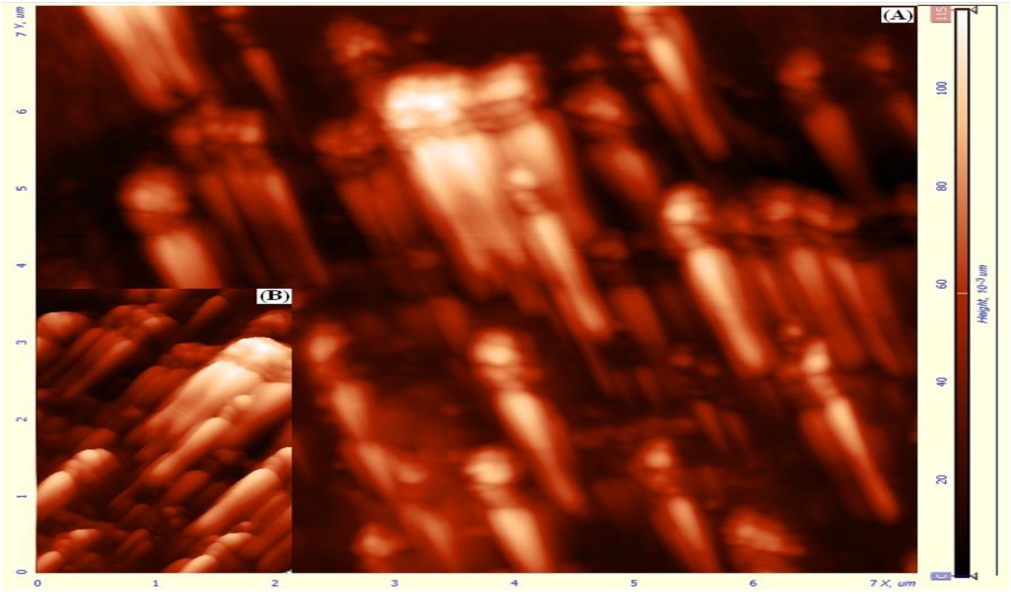


**Fig.2b.** 2D (A) and 3D (B) AFM micrograph of PTCDA thin film (at thickness of 470 nm as a representative example).

As observed from the Fig.2a, the plot showed that there is a single peak at 27.48ºcorresponding to (102) plane, a preferred orientation of growth. XRD pattern of PTCDA thin film is commonly described by a single peak (showing the preferred growth orientation) superimposed/dipped on the amorphous matrix. PTCDA crystal size was calculated using famous

Scherer's formula (Aydın et al., 2011; Cullity, 1978; Farag and Fadel, 2013; Shkir et al., 2012a; Shkir et al., 2012b) for the (102) plane:

$$L_{hkl} = \frac{0.9\lambda}{\beta \cos\theta}, \quad \textbf{(1)}$$

where $\lambda$ is wavelength of x-ray, $\beta$ is full width at half-maximum of the diffraction peak (in radians)and $\theta$ is the angular position of the diffraction peak. Rough size of the grain-like crystal of the PTCDA thin film of thickness 470 nm was then calculated and found to be 25.96 nm. Ludwing et al. [30] mentioned that PTCDA material can easily formed well-ordered layers on substrate due to its fine crystal structure.

2D and 3D surface morphology of the evaporated PTCDA thin film of thickness 470 nm was investigated using atomic force microscopy. The 2D and 3D AFM images of the film with dimension of 7x7 $\mu m^2$ are shown in Fig.2b. It is evident from the collected AFM data that the studied PTCDA film is composed of nano-rods. It is appeared as well that there are new growths of nano-particles at the top tip of these PTCDA rods.

## *3.2 Optical characterizations of PTCDA thin films.*

Studying optical properties of the investigated 3,4,9,10- Perylenetetracarboxylic dianhydride (PTCDA) films is important for obvious reasons. In particular, the investigation of the absorption edges of such material, which is crucial for understanding electronic structure and formation of any organic material. In the presented optical study, the spectral distribution of the refractive indices $n$ and absorption indices $k$ were obtained using the measured spectra of the transmittance and reflectance coefficients for the investigated PTCDA thin films. The onset energy gap $E_g$ and optical energy gap $E_g^{opt}$ are determined using the measured data of the absorption coefficients $\alpha$ of the films. The analysis of the refractive and distinction indices ($n$,$k$) was carried out to find real and imaginary parts of the complex dielectric functions ( $\varepsilon_1$ and $\varepsilon_2$ ), dissipation factors $\tan\delta$, VELF and SELF functions, and optical conductivity ( $\sigma_{opt}$ ).

### *3.2.1 Transmittance T(λ) and reflectance R(λ) spectra*

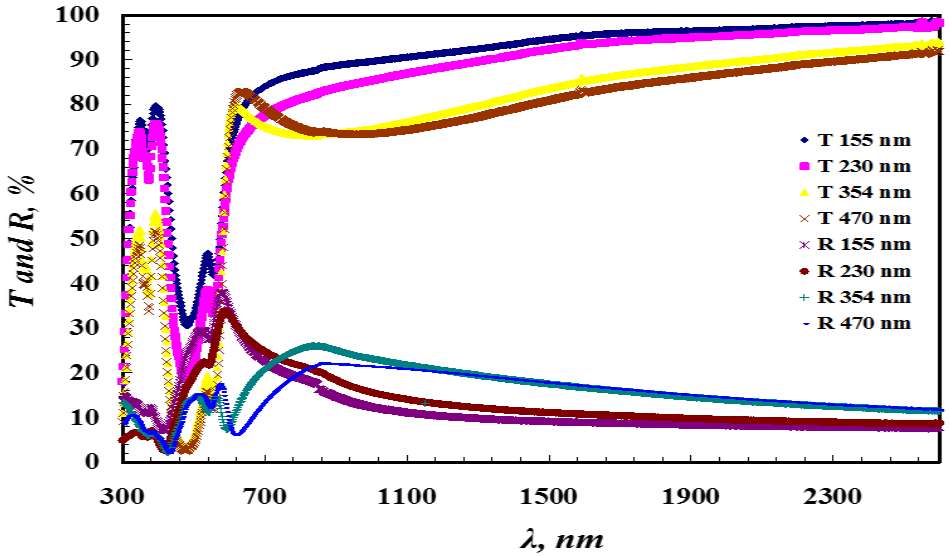


**Fig.3.** Spectral distribution of transmittance $T(\lambda)$ and reflectance $R(\lambda)$ of the PTCDA thin films of different thicknesses.

The spectral distribution of transmittance $T(\lambda)$ and reflectance $R(\lambda)$ coefficients was investigated for the PTCDA thin films of various thicknesses (155, 230, 354, and 470 nm) at normal incidence of light in the wavelength range 300- 2600 nm. Fig.3 depicts the obtained spectral curves of transmittance $T(\lambda)$ and reflectance $R(\lambda)$ for the PTCDA films, respectively. From the figure, one can note that at higher wavelengths all studied PTCDA films seem to be transparent and no scatting or absorption

of light due to the films in such region (i.e. $R+T=1$). Therefore, for this region it is possible to consider the absorption index to be dull($k=0$), then the refractive indices can be directly calculated. According to Fig.3, the absorption region for the films where inequality relation, $R+T<1$, holds is in shorter wavelengths.

### *3.2.2 The refractive and absorption (n,k) indices of the PTCDA films*

The obtained data from transmittance and reflectance measurements were used to compute the refractive and absorption indices using the following equations:

$$R=\left(\frac{(n-1)^2+k^2}{(n+1)^2+k^2}\right), \tag{2}$$

where normal reflectance of an absorbing material is usually calculated through equation (1) (Abelès, 1972; Caglar et al., 2009; Harbeke and Abeles, 1972; Hodgson, 1970). Then refractive index is then computed from the previous equation (Abelès, 1972; Yakuphanoglu et al., 2007a; Yakuphanoglu et al., 2007b) as:

$$n=\left(\frac{1+R}{1-R}\right)+\left(\frac{4R}{(1-R)^2}-k^2\right)^{1/2}, \tag{3}$$

where $n$ and $k$ are respectively refractive and absorption indices. While the values of the absorption indices $k$ are calculated from the absorption coefficients using the well-known relation of $k=\alpha\lambda/4\pi$ (Swanepoel, 1984), where $\alpha=A/t$ ($A$ is being the measured absorbance and $t$ is the thickness of the investigated film).The spectral distribution of $n$ and $k$ as functions of $\lambda$ for the PTCDA thin films deposited with varying thicknesses (155, 230, 354, 470 nm, and the average thickness values of these films) are plotted in Figs. (4&5), respectively. The*n* and *k* curves showed dependency on the film thickness.

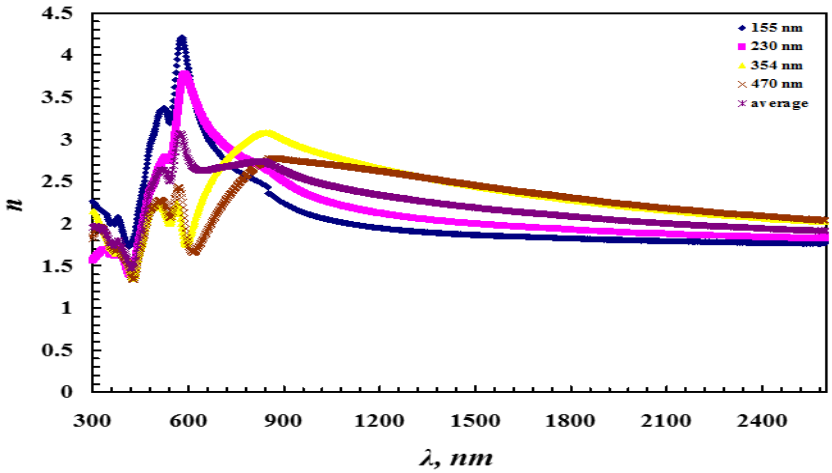


**Fig.4.**Dependency of the refractive indices *n* on the incident wavelengths for the PTCDA films deposited at various thicknesses.

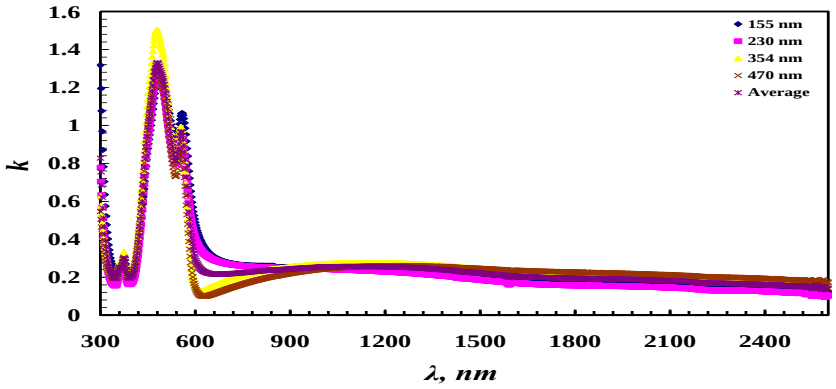


**Fig.5.** Dependency of the absorption indices *k* on the interacting wavelengths for the PTCDA thin films grown at different thicknesses.

### *3.2.3 Dielectric characterizations of the PTCDA films*

#### *3.2.3.1 Determination of high frequency dielectric constant $\varepsilon_\infty$.*

High frequency dielectric constant $\varepsilon_\infty$ can be estimated by analyzing the obtained data of the refractive indices. $\varepsilon_\infty$ is commonly associated with the free carriers and lattice vibration modes of the material dispersion properties (Mahmoud et al., 2011). In addition, $\varepsilon_\infty$ can be related to the material refractive index through the following equation: (El-Nahass et al., 2011a; Mahmoud et al., 2011):

$$\varepsilon_1 = n^2 = \varepsilon_\infty - \frac{e^2 N}{4\pi^2 c^2 \varepsilon_o m^*}\lambda^2 \quad \textbf{(4)}$$

Where $\varepsilon_1$ is real part of dielectric function, *e* is the elementary electron charge, *N* is concentration of free charge carriers, $\varepsilon_o$ is free space permittivity = $8.854\times10^{-12} F/m$, where $m^*$ is effective mass of charge carrier and $c$ is the speed constant of light.The relation between $\varepsilon_1 = n^2$ and $\lambda^2$ for PTCDA thin films studied in this presented work is shown in Fig.6.

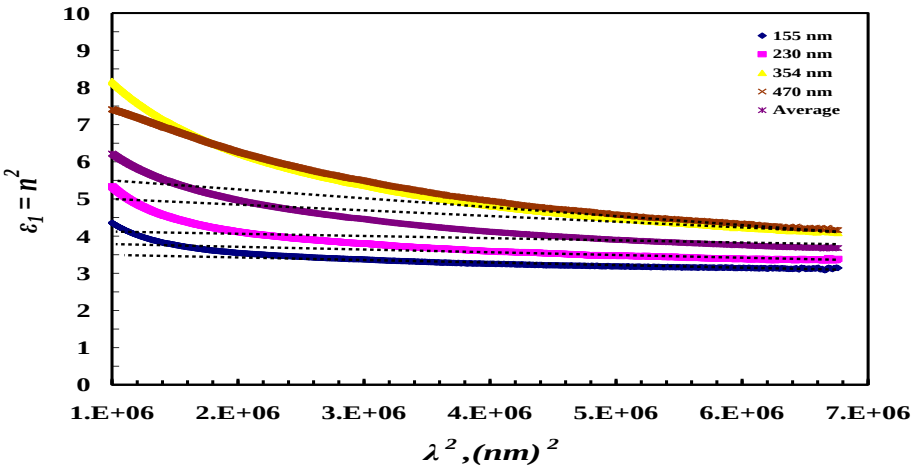


**Fig.6.** Plots of $\varepsilon_1 = n^2$ as a function of $\lambda^2$ for the PTCDA thin films of different thicknesses.

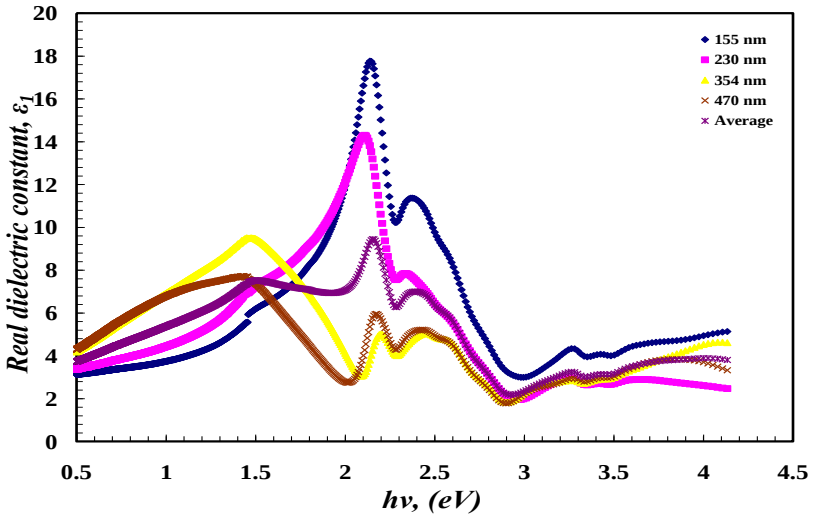


**Fig. 7.** Plots of $\varepsilon_1$ vs. photon energy ($h\upsilon$) for the PTCDA thin films at different thicknesses.

It is clear that there is a dependency of $\varepsilon_1$ on $\lambda^2$, which is linear at higher wavelengths. This verifies the linearity of Eq.(3). Value of $\varepsilon_\infty$ for each thin film is then determined from extrapolation to the linear part of the plot to $\lambda^2 = 0$ and the corresponding values of $N/m^*$ were calculated from the graphs slopes. The values of $\varepsilon_\infty$ are 3.50, 3.75, 5.00, 5.50, and 4.15 for PTCDA thin films with thicknesses 155, 230, 354, 470 nm, and its average, respectively. Taking into account that $\varepsilon_\infty \approx \varepsilon_L$, where $\varepsilon_L$ is lattice dielectric constant. In addition, it is important to notice that at high frequency the localized traps in a material cannot be followed by its optical signals. Hence, the contribution of the charge carrier may be neglected(El-Nahass et al., 2011a; Farag and Yahia, 2010).

### *3.2.3.2 Determination of real part $\varepsilon_1$ and imaginary part $\varepsilon_2$ of dielectric function*

Studying dispersion behaviors of a dielectric function ($\hat{\varepsilon}$) gives researcher an important tool to understand light reflection, refraction, and dissipation in multilayer materials. Moreover, such approach can eventually shed light on the electronic structure of the material under investigation. In fact, $\hat{\varepsilon}$ is considered an important physical quantity when designing effective optoelectronic devices (Abdel-Aziz et al., 2006; El-Korashy et al., 2003; Fadel et al., 2009;Khan et al., 2010). $\hat{\varepsilon} = \varepsilon_1(\lambda) + i\varepsilon_2(\lambda)$ asa function of wavelength has real part $\varepsilon_1$, representing the normal dielectric constant, and an imaginary part $\varepsilon_2$, corresponding to absorption associated with the media free carrier radiation. For the studied PTCDA films, the dielectric function parts are determined by the following relations at the material light absorption region, where $k \neq 0$ (Abdel-Aziz et al., 2006; El-Korashy et al., 2003; Fadel et al., 2009; Khan et al., 2010):

$$\varepsilon_1 = n^2 - k^2 = \varepsilon_\infty - \left(\frac{e^2 N}{4\pi c^2 \varepsilon_0 m^*}\right)\lambda^2, \quad \textbf{(5)}$$

and

$$\varepsilon_2 = 2nk = \left(\frac{\varepsilon_\infty \omega_p^2}{8\pi^2 c^3 \tau}\right)\lambda^3, \quad \textbf{(6)}$$

where $\tau$ is relaxation time, $k = \alpha\lambda/4\pi$ is extinction coefficient and $\omega_p = 2\pi\upsilon$ is photon angular frequency. The dependences of $\varepsilon_1$ and $\varepsilon_2$ on light energy ($h\upsilon$) for the studied PTCDA films grown with various thicknesses are plotted in Figs.(7&8), respectively. Apparently, real parts of PTCDA films dielectric function have higher values than those of the imaginary ones, although they are both (real and imaginary parts) behaving in a similar pattern. In general, variation of the PTCDA dielectric function with varying photon energy is a sign of photon-electron interactions taking places within the

PTCDA material at the covered energy range (Abdel-Aziz et al., 2006; El-Korashy et al., 2003; Fadel et al., 2009; Khan et al., 2010).

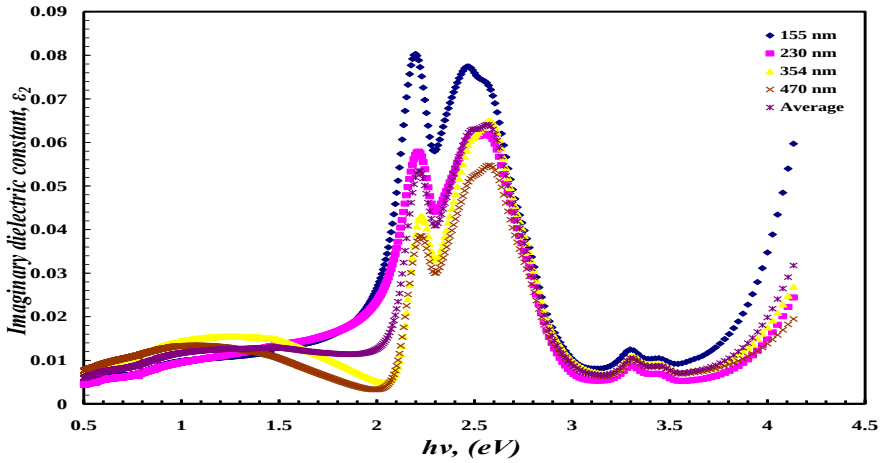


**Fig.8.** Plots of $\varepsilon_2$ vs. photon energy ($h\upsilon$) for the PTCDA thin films of varying thicknesses.

Real and Imaginary parts of a dielectric function are usually used to find out the dissipation factor ($\tan\delta$) of a material. Since $\tan\delta$ can be defined as the rate of a power loss in an oscillation mode for dissipative systems. Hence, dissipation factor $\tan\delta$ in a material system is known as the ratio of the absorption due to the free charge carriers in the system to the normal dielectric constant of the system and it can be computed from the following equation (Fadel et al., 2009):

$$\tan\delta = \frac{\varepsilon_2}{\varepsilon_1} \tag{7}$$

The dissipation factor $\tan\delta$ of the studied PTCDA thin films is calculated and shown in Fig.9. Observation from Fig.9 suggests patterns similarity of $\tan\delta$ and dielectric function of the studied PTCDA films. Such observation is also supporting the idea of active electron-photon interactions taking place within the PTCDA film's material at the investigated energy range.

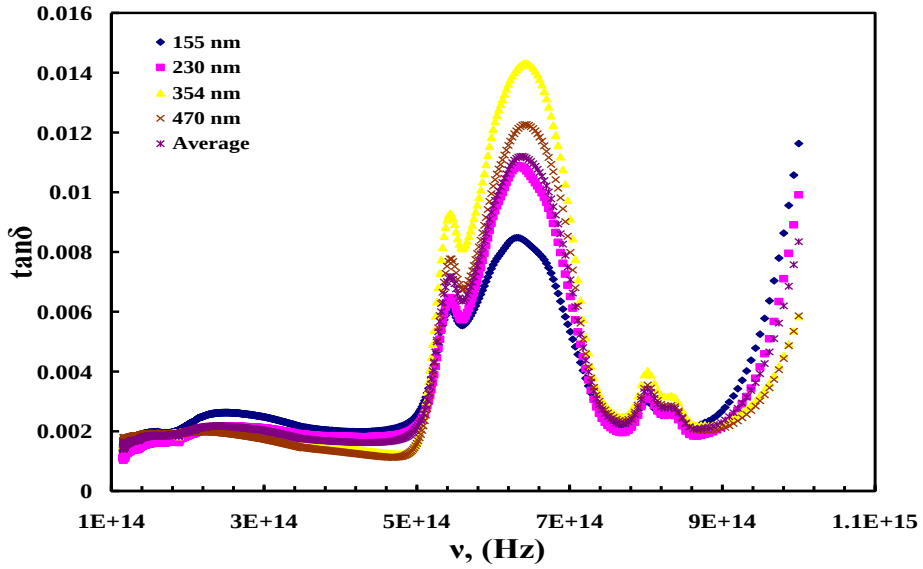


**Fig.9.** The variation of the dissipation factor $\tan\delta$ for the PTCDA thin films with the photon energy ($h\upsilon$).

Table. 1 Energy band gap values and their mean (average) values for the PTCDA films grown at different thicknesses.

| **Thickness** | $E_{g1}$,(eV) | $E_{g2}$,(eV) | $E_{g3}$,(eV) | $E_{g4}$, (eV) |
|---|---|---|---|---|
| 155 nm | 1.84 | 1.70 | 2.80 | 3.45 |
| 230 nm | 1.95 | 1.72 | 2.82 | 3.50 |
| 354 nm | 2.2 | 1.90 | 2.80 | 3.40 |
| 470 nm | 2.2 | 1.92 | 2.80 | 3.40 |
| average | 1.88 | 1.95 | 2.70 | 3.45 |

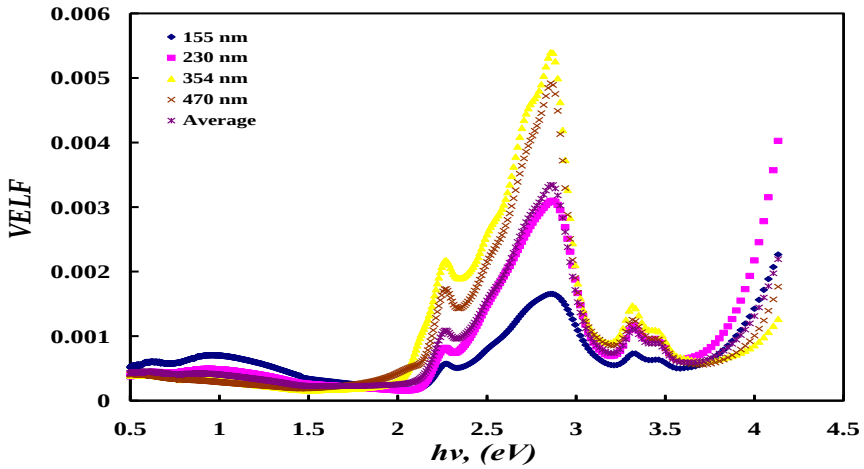


**Fig.10.** Dependency of *VELF* on the photon energy ($h\upsilon$) for the PTCDA thin films.

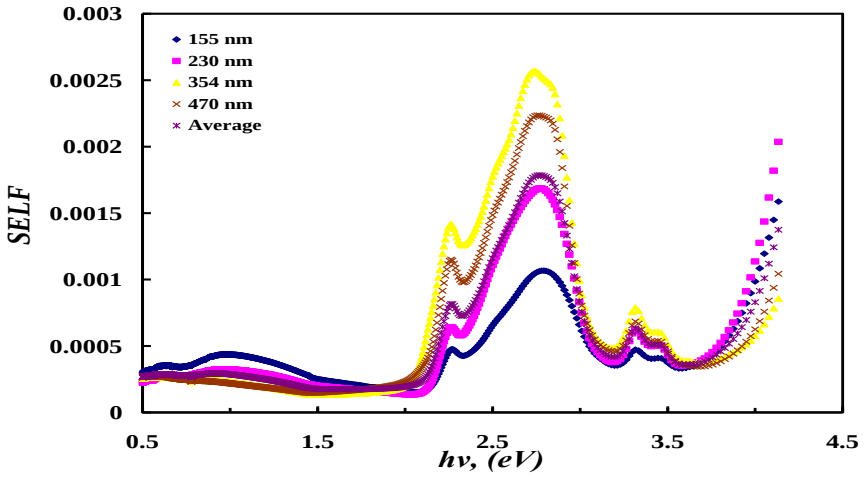


**Fig. 11.** Dependency of the *SELF* on the photon energy ($h\upsilon$) for the PTCDA thin films grown at different thicknesses.

### *3.2.3.3 Determination of VELF and SELF for the PTCDA film*

In this section, the interest is to study some physical quantities of the PTCDA film. They are commonly used to describe the rate of electron energy loss when passing through a material. These quantities are the volume energy loss (*VELF*) and the surface energy loss (*SELF*) functions. VELF and SELF can be related to the real and imaginary terms of a dielectric function as well through the following relation (Farag and Yahia, 2010; Mahmoud et al., 2011):

$$VELF = -\mathrm{Im}\left(\frac{1}{\hat{\varepsilon}}\right) = \frac{\varepsilon_2}{\varepsilon_1^2 + \varepsilon_2^2}, \tag{8}$$

and

$$SELF = -\mathrm{Im}\left(\frac{1}{\hat{\varepsilon}+1}\right) = \left(\frac{\varepsilon_2}{(\varepsilon_1+1)^2 + \varepsilon_2^2}\right), \tag{9}$$

Figs.(10&11) respectively presented *VELF* and *SELF* of the investigated PTCDA films as functions in photon energies. From these figures, It is can be concluded that the functions of energy loss of the transporting free charge carriers, when traversing through the PTCDA's bulk or when traversing the PTCDA's surface, are behaving in similar ways, especially in lower energy regions. There is no significant difference between VELF and SELF of the studied PTCDA films at lower and higher photon energies. However, it seems that values of VELF are increasing more rapidly than that of SELF at particular peaks.

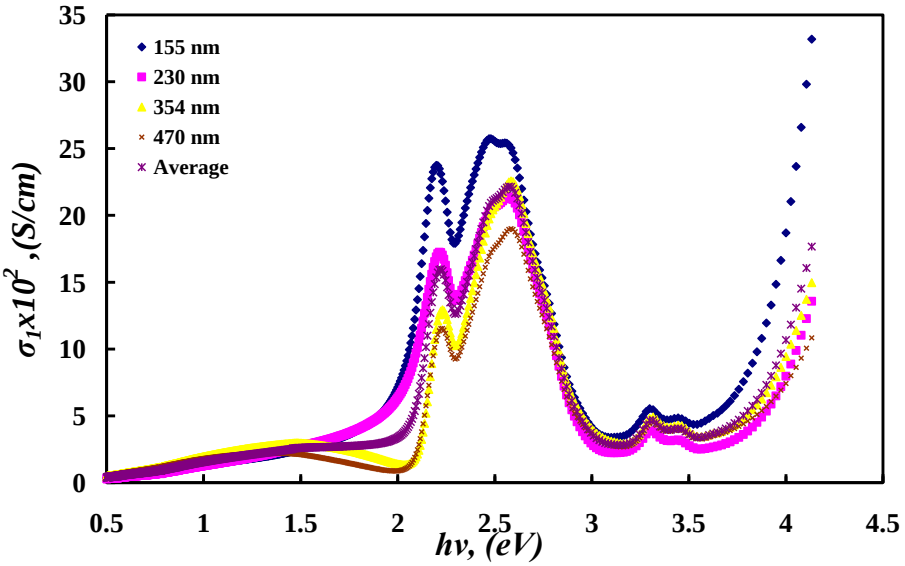


**Fig.12.** Dependency of $\sigma_1$ on the photon energy ($h\upsilon$) for the PTCDA thin films.

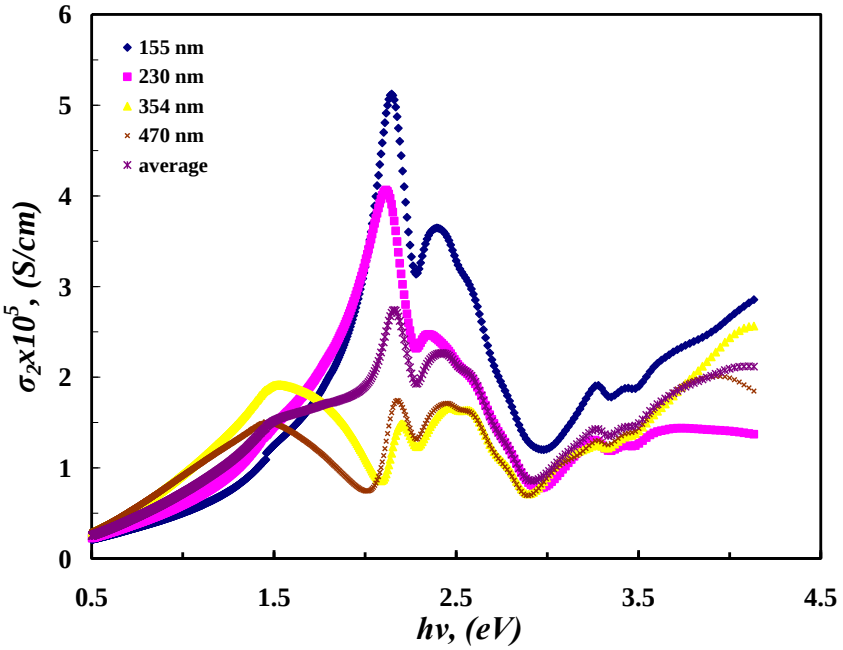


**Fig.13.** Dependency of $\sigma_2$ the photon energy ($h\upsilon$) for the PTCDA thin films deposited with different thicknesses.

### *3.2.4 Optical conductivity of PTCDA films*

Optical conductivity $\sigma_{opt}$ is one of the fundamental properties of a material, it sums its optical properties. In general, the optical conductivity of a material is used to learn aboutthe material's allowed inter-band for optical transitions. The complex optical conductivity ($\hat{\sigma} = \sigma_1(\lambda) + i\sigma_2(\lambda)$) of a material is in fact connected to its dielectric function ($\hat{\varepsilon} = \varepsilon_1(\lambda) + i\varepsilon_2(\lambda)$) through following relations (Yakuphanoglu et al., 2004):

$$\sigma_1 = \omega\varepsilon_2\varepsilon_0, \qquad \text{and } \sigma_2 = \omega\varepsilon_1\varepsilon_0, \tag{10}$$

where $\sigma_1$ and $\sigma_2$ are respectively real and imaginary parts of the material's optical conductivity . Figs.(12&13) show $\sigma_1(h\upsilon)$ and $\sigma_2(h\upsilon)$ functions for the studied films of PTCDA grown with varying thicknesses. The results exhibit crisscross relations between imaginary and real parts of the PTCDA's optical conductivity and dielectric function. The real parts of the optical conductivity and the imaginary ones of the film's dielectric function and vice versa were found following the same patterns, for comparison see Figs.(7&8) and Figs.(12&13). The results showed as well that there are four distinct peaks for $\sigma_1$ and $\sigma_2$, origin of such peaks can be attributed to optical inter-band transitions within the studied material(Yakuphanoglu et al., 2004).

### *3.2.5 Energy gap determination*

Knowledge of the spectral distribution of the absorption coefficients of a semiconductor material near fundamental edge is important to understand the types and behavior of the material's optical transitions (direct and indirect transitions). Such knowledge is also valuable when studying the material's band gap structure. Utilizing Maxwell equations, the material's absorption coefficient ($\alpha$) is calculated from the equation, $\alpha = \frac{4\pi k}{\lambda}$, where *k* is distinction constant and $\lambda$ is the optical wavelength. The optical band gap and transitions, for the material under investigation, are then obtained from the absorption coefficients as functions on photon energy ($h\upsilon$) (El-Nahass et al., 2004a; El-Nahass et al., 2004b; Kamath et al., 2002).In general, the absorption spectrum of an organic material does follow a power-law equation (Azim et al., 2009; Mahmoud et al., 2011; Pal et al., 1993; Yaghmour, 2009; Yakuphanoglu, 2009):

$$\alpha h\upsilon = A\left(h\upsilon - E_g\right)^m, \tag{11}$$

where $\alpha$ is the absorbance coefficient, $E_g$ is optical band gap energy, and *A* is a constant (independent of $h\upsilon$ but depends on transition probability). *m* is a specific number of transition process (direct or indirect). In this work, the indirect band gap transitions of the studied film was estimated through plotting $(\alpha h\upsilon)^{1/2}$ versus ($h\upsilon$) with *m*=2, and through extrapolation of the linear part of the resulted curve at the lower energy limit. Fig.14a shows the dependency of $(\alpha h\upsilon)^{1/2}$ on ($h\upsilon$) for the PTCDA thin films deposited at various thicknesses. For simplicity, Fig.14b shows the band gap structures of only one curve from the results showed in Fig.14a, which is a characterization for the average result of the thin films.

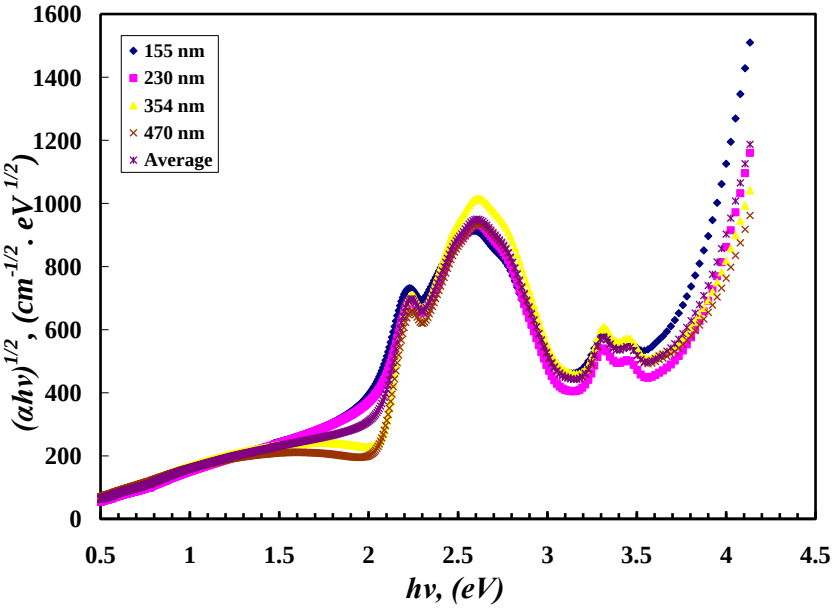


**Fig. 14a.** Plots of $(\alpha h\upsilon)^{1/2}$ vs. photon energy ($h\upsilon$) for the PTCDA thin films.

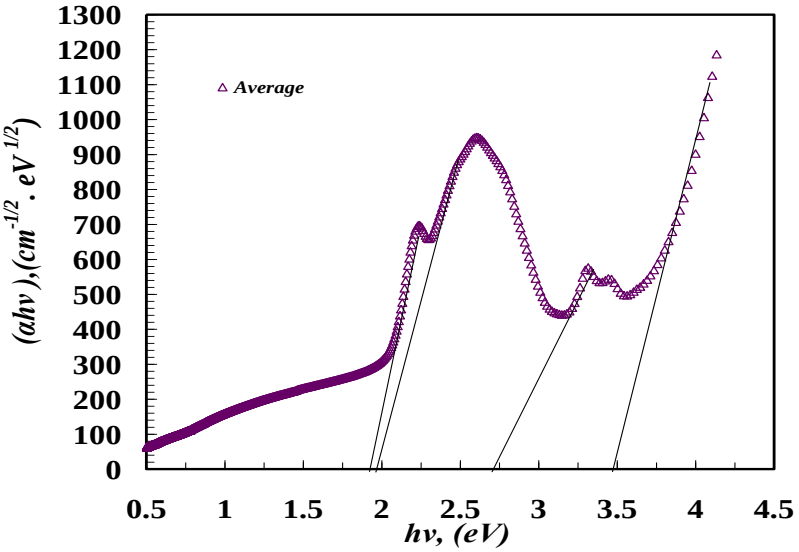


**Fig.14b.** Energy band gap structure plot of the average of $(\alpha h\upsilon)^{1/2}$ vs. photon energy ($h\upsilon$) for of the PTCDA thin films at average thickness.

Each thickness of the studied organic films has at least four indirect energy gap bands; their values are found to be 1.88, 1.95, 2.70, and 3.45eV,respectively.The found transitions of the studied films are in well agreement with earlier work(Collins et al., 1993; El-Nahass et al., 2011b; El-Nahass and Youssef, 2010; Kumar et al., 2000) on PTCDA. It should be noted though that the first founded energy's value is the optical energy band gap $E_g^{opt}$ of the studied material. $E_g^{opt}$ does correspond to the onset of the optical absorption and formation of the bound electron-hole pair (Frenkel exciton) (Tsiper et al., 2002). However, the last energy value is the fundamental energy gap (gap between valence $\pi$ and conduction $\pi^*$ bands) (Zhokhavets et al., 2003). The values in between may be attributed to impurities in the material.

## 4 Conclusion

The XRD analysis of the PTCDA film confirms its nanostructure morphology with crystalline size of 25.96 nm. In addition, the nanostructure of the PTCDA film material was characterized by a preferred orientation along (102 ) plane. The AFM supports the results of the XRD showing a nanostructure of the studied film with grain (nanoparticles) size of ~44.56 nm and surface roughness of ~11.599 nm. The obtained values of $n$ and $k$ constants of the PTCDA film were found to be dependent on the films thickness. The real and imaginary constants of the films dielectric function behave in similar patterns when compared to their corresponding optical constants. In addition, for the PTCDA film, the dielectric function's real parts are of higher values than those of the imaginary ones. It seems that there are some photon-electron interactions taking place within the PTCDA film material over the studied range of wavelengths according to the depicted variation of the film dielectric function at varying photon energy. The dissipation factor $\tan\delta$ for the PTCDA film showed dependency on the film's thickness. The energy loss function of the free charge carriers traversing through the bulk of the PTCDA material was found to have the same behavior as when these charges traversing the surface of the PTCDA film, in particular at the relativity lower energy's regions. However, the values of the *VELF* increase more rapidly than those of the SELF at particular peaks, which characterized the film PTCDA material. For the PTCDA films subjected to this work, it was found that the values of the real part of the film's optical conductivity $\sigma_1$ and the imaginary ones of its dielectric function $\varepsilon_2$ follow the same pattern. These energy gaps are from 1.88 eV to 3.45 eV with the first energy gap value corresponds to the optical band gap energy $E_g^{opt}$ of the film. The characteristic band gap structure of the PTCDA film seems to fit in general with the standard behavior of the indirect optical transitions within organic semiconductor materials.

1. ).

## References


[1] Abdel-Aziz, M., Yahia, I., Wahab, L., Fadel, M., Afifi, M., 2006. Determination and analysis of dispersive optical constant of TiO 2 and Ti 2 O 3 thin films. Applied Surface Science 252, 8163-8170.

[2] Abelès, F., 1972. Optical properties of solids.

[3] Aydın, C., El-Nasser, H., Yakuphanoglu, F., Yahia, I., Aksoy, M., 2011. Nanopowder synthesis of aluminum doped cadmium oxide via sol–gel calcination processing. Journal of Alloys and Compounds 509, 854-858.

[4] Azim, O.A., Abdel-Aziz, M., Yahia, I., 2009. Structure and optical analysis of Ta 2 O 5 deposited on infrasil substrate. Applied Surface Science 255, 4829-4835.

[5] Bayliss, S., Heutz, S., Rumbles, G., Jones, T., 1999. Effect of Annealing on the Properties of thin Films of Free Base Phthalocyanine and Perylene-3, 4, 9, 10-Tetracarboxylic Dianhydride Deposited by Organic Molecular Beam Deposition, MRS Proceedings. Cambridge Univ Press, p. 71.

[6] Böhler, A., Urbach, P., Schöbel, J., Dirr, S., Johannes, H.-H., Wiese, S., Ammermann, D., Kowalsky, W., 1998. Organic heterostructures for electronic and photonic devices. Physica E: Low-dimensional Systems and Nanostructures 2, 562-572.

[7] Borsenberger, P.M., 1998. Organic photoreceptors for xerography. CRC Press.

[8] Briseno, A.L., Mannsfeld, S.C., Reese, C., Hancock, J.M., Xiong, Y., Jenekhe, S.A., Bao, Z., Xia, Y., 2007. Perylenediimide nanowires and their use in fabricating field-effect transistors and complementary inverters. Nano letters 7, 2847-2853.

[9] Bulović, V., Burrows, P., Forrest, S., Cronin, J., Thompson, M., 1996. Study of localized and extended excitons in 3, 4, 9, 10-perylenetetracarboxylic dianhydride (PTCDA) I. Spectroscopic properties of thin films and solutions. Chemical Physics 210, 1-12.

[10] Caglar, M., Ilican, S., Caglar, Y., Yakuphanoglu, F., 2009. Electrical conductivity and optical properties of ZnO nanostructured thin film. Applied Surface Science 255, 4491-4496.

[11] Chen, Z., Stepanenko, V., Dehm, V., Prins, P., Siebbeles, L.D., Seibt, J., Marquetand, P., Engel, V., Wuerthner, F., 2007.

Photoluminescence and Conductivity of Self-Assembled π–π Stacks of Perylene Bisimide Dyes. Chemistry-a European Journal 13, 436-449.

[12] Collins, R.A., Krier, A., Abass, A.K., 1993. Optical properties of lead phthalocyanine (PbPc) thin films. Thin Solid Films 229, 113-118.

[13] Cullity, B., 1978. Elements of X–ray Diffraction. Addison-Wesley, Reading, MA.

[14] Djurišić, A.B., Fritz, T., Leo, K., 2000. Modeling the optical constants of organic thin films: application to 3, 4, 9, 10-perylenetetracarboxylic dianhydride (PTCDA). Optics Communications 183, 123-132.

[15] El-Korashy, A., El-Zahed, H., Radwan, M., 2003. Optical studies of [N(CH3)4]2CoCl4, [N(CH3)4]2MnCl4 single crystals in the normal paraelectric phase. Physica B: Condensed Matter 334, 75-81.

[16] El-Nahass, M., Abd-El-Rahman, K., Farag, A., Darwish, A., 2004a. Optical characterisation of thermally evaporated nickel phthalocyanine thin films. International Journal of Modern Physics B 18, 421-434.

[17] El-Nahass, M., Ammar, A., Atta, A., Farag, A., El-Zaidia, E., 2011a. Influence of X-ray irradiation on the optical properties of CoMTPP thin films. Optics Communications 284, 2259-2263.

[18] El-Nahass, M., Ammar, A., Farag, A., Atta, A., El-Zaidia, E., 2011b. Effect of heat treatment on morphological, structural and optical properties of CoMTPP thin films. Solid State Sciences 13, 596-600.

[19] El-Nahass, M.M., Abd-El-Rahman, K.F., Al-Ghamdi, A.A., Asiri, A.M., 2004b. Optical properties of thermally evaporated tin-phthalocyanine dichloride thin films, SnPcCl2. Physica B: Condensed Matter 344, 398-406.

[20] El-Nahass, M.M., Youssef, T.E., 2010. Influence of X-ray irradiation on the optical properties of ruthenium(II)octa-(n-hexyl)-phthalocyanine thin film. Journal of Alloys and Compounds 503, 86-91.

[21] Fadel, M., Fayek, S., Abou-Helal, M., Ibrahim, M., Shakra, A., 2009. Structural and optical properties of SeGe and SeGeX (X= In, Sb and Bi) amorphous films. Journal of Alloys and Compounds 485, 604-609.

[22] Farag, A., Fadel, M., 2013. Optical absorption and dispersion analysis of nanocrystalline perylene-3, 4, 9, 10-tetracarboxylic-3, 4, 9, 10-dianhydride film prepared by dip coating and its optoelectronic application. Optics & Laser Technology 45, 356-363.

[23] Farag, A., Yahia, I., 2010. Structural, absorption and optical dispersion characteristics of rhodamine B thin films prepared by drop casting technique. Optics Communications 283, 4310-4317.

[24] Fenter, P., Schreiber, F., Zhou, L., Eisenberger, P., Forrest, S., 1997. In situ studies of morphology, strain, and growth modes of a molecular organic thin film. Physical Review B 56, 3046.

[25] Forrest, S.R., 1997. Ultrathin Organic Films Grown by Organic Molecular Beam Deposition and Related Techniques. Chemical Reviews 97, 1793-1896.

[26] Friedrich, M., Wagner, T., Salvan, G., Park, S., Kampen, T., Zahn, D., 2002. Optical constants of 3, 4, 9, 10-perylenetetracarboxylic dianhydride films on silicon and gallium arsenide studied by spectroscopic ellipsometry. Applied Physics A 75, 501-506.

[27] Harbeke, G., Abeles, F., 1972. Optical properties of solids. North-Holland, Amsterdam.

[28] Hodgson, J.N., 1970. Optical absorption and dispersion in solids. CRC Press.

[29] Hoeben, F.J., Jonkheijm, P., Meijer, E., Schenning, A.P., 2005. About supramolecular assemblies of π-conjugated systems. Chemical Reviews 105, 1491-1546.

[30] Jones, B.A., Facchetti, A., Wasielewski, M.R., Marks, T.J., 2007. High Mobility Air-Stable n-Type Perylene Diimide Semiconductors. Insight Into Materials Design for Stability of n-Type Charge Transport. J. Am. Chem. Soc 129, 15259-15278.

[31] Kamath, G.B., Joseph, C., Menon, C., 2002. Effect of air annealing on the electrical and optical properties of MgPc thin films. Materials Letters 57, 730-733.

[32] Karmann, E., Meyer, J.-P., Schlettwein, D., Jaeger, N., Anderson, M., Schmidt, A., Armstrong, N., 1996. Photoelectrochemical effects and (photo) conductivity of "n-type" phthalocyanines. Molecular Crystals and Liquid Crystals 283, 283-291.

[33] Khan, S.A., Al-Hazmi, F., Al-Heniti, S., Faidah, A., Al-Ghamdi, A., 2010. Effect of cadmium addition on the optical constants of thermally evaporated amorphous Se–S–Cd thin films. Current Applied Physics 10, 145-152.

[34] Kumar, G., Thomas, J., George, N., Kumar, B., Radhakrishnan, P., Nampoori, V., Vallabhan, C., Unnikrishnan, N., 2000. Optical absorption studies of free (H2Pc) and rare earth (RePc) phthalocyanine doped borate glasses. Physics and Chemistry of Glasses-European Journal of Glass Science and Technology Part B 41, 89-93.

[35] Law, K.Y., 1993. Organic photoconductive materials: recent trends and developments. Chemical Reviews 93, 449-486.

[36] Lee, S., Hong, S.I., Shim, H.-K., Lee, C., 1998. PTCDA/PPET heterostructure light emitting diode. Molecular Crystals and Liquid

Crystals 316, 289-292.

[37] Leonhardt, M., Mager, O., Port, H., 1999. Two-component optical spectra in thin PTCDA films due to the coexistence of α-and β-phase. Chemical Physics Letters 313, 24-30.

[38] Mahmoud, S.A., Shereen, A., Mou'ad, A.T., 2011. Structural and Optical Dispersion Characterisation of Sprayed Nickel Oxide Thin Films. Journal of Modern Physics 2011.

[39] Möbus, M., Karl, N., Kobayashi, T., 1992. Structure of perylene-tetracarboxylic-dianhydride thin films on alkali halide crystal substrates. Journal of crystal growth 116, 495-504.

[40] Nagaseki, K., Ishikawa, I., Nishimura, E., Saito, Y., Suganomata, S., 1995. Negative Ions in 13.56 MHz discharge of SF6 gas in a Planar Diode. Japanese journal of applied physics 34, L852.

[41] Oukachmih, M., Destruel, P., Seguy, I., Ablart, G., Jolinat, P., Archambeau, S., Mabiala, M., Fouet, S., Bock, H., 2005. New organic discotic materials for photovoltaic conversion. Solar energy materials and solar cells 85, 535-543.

[42] Pal, U., Samanta, D., Ghorai, S., Chaudhuri, A., 1993. Optical constants of vacuum-evaporated polycrystalline cadmium selenide thin films. Journal of Applied Physics 74, 6368-6374.

[43] Schmitz-Hübsch, T., Fritz, T., Sellam, F., Staub, R., Leo, K., 1997. Epitaxial growth of 3, 4, 9, 10-perylene-tetracarboxylic-dianhydride on Au (111): A STM and RHEED study. Physical Review B 55, 7972.

[44] Shen, Z., Burrows, P.E., Bulović, V., Forrest, S.R., Thompson, M.E., 1997. Three-color, tunable, organic light-emitting devices. Science 276, 2009-2011.

[45] Shkir, M., Aarya, S., Singh, R., Arora, M., Bhagavannarayana, G., Senguttuvan, T., 2012a. Synthesis of ZnTe Nanoparticles by Microwave Irradiation Technique, and Their Characterization. Nanoscience and Nanotechnology Letters 4, 405-408.

[46] Shkir, M., Abbas, H., Khan, Z.R., 2012b. Effect of thickness on the structural, optical and electrical properties of thermally evaporated PbI< sub> 2</sub> thin films. Journal of Physics and Chemistry of Solids 73, 1309-1313.

[47] Swanepoel, R., 1984. Determination of surface roughness and optical constants of inhomogeneous amorphous silicon films. Journal of Physics E: Scientific Instruments 17, 896.

[48] Taylor, R.B., Burrows, P.E., Forrest, S.R., 1997. An integrated, crystalline organic waveguide-coupled InGaAs photodetector. Photonics Technology Letters, IEEE 9, 365-367.

[49] Tsiper, E., Soos, Z., Gao, W., Kahn, A., 2002. Electronic polarization at surfaces and thin films of organic molecular crystals: PTCDA. Chemical Physics Letters 360, 47-52.

[50] Urbach, P., Felbier, F., Sörensen, A., Kowalsky, W., 1998. Organic-on-inorganic heterostructure diodes for microwave applications. Japanese journal of applied physics 37, 1660.

[51] Würthner, F., Thalacker, C., Diele, S., Tschierske, C., 2001. Fluorescent J-type Aggregates and Thermotropic Columnar Mesophases of Perylene Bisimide Dyes. Chemistry-a European Journal 7, 2245-2253.

[52] Yaghmour, S.J., 2009. Influence of γ-irradiation on optical properties of manganese phthalocyanine thin films. Journal of Alloys and Compounds 486, 284-287.

[53] Yakuphanoglu, F., 2009. Electrical conductivity, Seebeck coefficient and optical properties of SnO2 film deposited on ITO by dip coating. Journal of Alloys and Compounds 470, 55-59.

[54] Yakuphanoglu, F., Barım, G., Erol, I., 2007a. The effect of FeCl 3 on the optical constants and optical band gap of MBZMA-co-MMA polymer thin films. Physica B: Condensed Matter 391, 136-140.

[55] Yakuphanoglu, F., Kandaz, M., Yaraşır, M., Şenkal, F., 2007b. Electrical transport and optical properties of an organic semiconductor based on phthalocyanine. Physica B: Condensed Matter 393, 235-238.

[56] Yakuphanoglu, F., Sekerci, M., Ozturk, O.F., 2004. The determination of the optical constants of Cu(II) compound having 1-chloro-2,3-o-cyclohexylidinepropane thin film. Optics Communications 239, 275-280.

[57] Zang, D., So, F., Forrest, S., 1991. Giant anisotropies in the dielectric properties of quasi-epitaxial crystalline organic semiconductor thin films. Applied Physics Letters 59, 823-825.

[58] Zhokhavets, U., Goldhahn, R., Gobsch, G., Schliefke, W., 2003. Dielectric function and one-dimensional description of the absorption of poly (3-octylthiophene). Synthetic Metals 138, 491-495.